Structural Characterization of Charcoal Exposed to High and Low pH: Implications for 14C Sample Preparation and Charcoal Preservation

RADIOCARBON, Vol 50, Nr 2, 2008, p 289–307

STRUCTURAL CHARACTERIZATION OF CHARCOAL EXPOSED TO HIGH AND LOW pH: IMPLICATIONS FOR ^{14}C SAMPLE PREPARATION AND CHARCOAL PRESERVATION

N R Rebollo[1] • I Cohen-Ofri[2] • R Popovitz-Biro[3] • O Bar-Yosef[4] • L Meignen[5] • P Goldberg[6] • S Weiner[2] • E Boaretto[1,7]

ABSTRACT. Chemical and structural similarities between poorly preserved charcoal and its contaminants, as well as low radiocarbon concentrations in old samples, complicate ^{14}C age determinations. Here, we characterize 4 fossil charcoal samples from the late Middle Paleolithic and early Upper Paleolithic strata of Kebara Cave, Israel, with respect to the structural and chemical changes that occur when they are subjected to the acid-base-acid (ABA) treatment. Differential thermal analysis and TEM show that acid treatment disrupts the structure, whereas alkali treatment results in the reformation of molecular aggregates. The major changes are ascribed to the formation of salt bridges at high pH and the disruption of the graphite-like crystallites at low pH. Weight losses during the treatments are consistently greater for older samples, implying that they are less well preserved. Based on the changes observed *in vitro* due to pH fluctuations, various methods for removing contamination, as well as a mechanism for preferential preservation of charcoal in nature, are proposed.

INTRODUCTION

Charcoal is commonly used for radiocarbon dating, especially in relatively old samples where the "old wood" effect (Schiffer 1986; Taylor 1987) is less relevant. The older the sample, the less ^{14}C is present, and hence contamination from other materials significantly alters the date obtained. Furthermore, as charcoal is not stable over time, old charcoal samples are less well preserved (Frink 1992; Bird et al. 2002). Cohen-Ofri et al. (2006, 2007) have suggested that the relative proportions of graphite-like crystallites decrease in fossil charcoal as compared to modern charcoal, whereas the non-organized structure increases. They also noted that fossil charcoal undergoes oxidation to form carboxylate groups (Cohen-Ofri et al. 2006). This results in components of the charcoal becoming more soluble, especially under high pH conditions. They thus tend to resemble humic substances. Consequently, it is more difficult to remove relatively soluble contaminants (also mainly humic substances) from poorly preserved charcoal, as the charcoal components themselves tend to dissolve. In addition, this loss of charcoal may result in the enrichment of other components such as clay containing adsorbed organic materials. Dating such charcoal will result in an erroneous age, as was observed in the case of some of the samples from Motza, Israel (Yizhaq et al. 2005). It is therefore a challenge to accurately date poorly preserved charcoal.

The method commonly used for removing contaminants from charcoal samples is the so-called acid-base-acid (ABA) pretreatment (Olson and Broecker 1958). The basic ideas behind this treatment are that the initial acid treatment primarily removes soluble carbonates and other minerals; the alkali treatment removes the humic substances; and the final acid treatment removes the dissolved carbon dioxide. The exact manner in which these treatments are applied is for the most part empirical. In many laboratories, for example, successive treatments with alkali are applied until the supernatant is colorless or almost colorless (Sakamoto et al. 2004). Furthermore, the concentrations of

[1]Radiocarbon Dating and Cosmogenic Isotopes Laboratory, Kimmel Center for Archaeological Science, Weizmann Institute of Science, Rehovot 76100, Israel.
[2]Department of Structural Biology, Weizmann Institute of Science, Rehovot 76100, Israel.
[3]Chemical Research Support Unit, Weizmann Institute of Science, Rehovot 76100, Israel.
[4]Department of Anthropology, Peabody Museum, Harvard University, Cambridge 02138, Massachusetts, USA.
[5]UNSA, CEPAM-CNRS, Sophia Antipolis, 06560 Valbonne, France.
[6]Department of Archaeology, Boston University, 675 Commonwealth Avenue, Boston 02215, Massachusetts, USA.
[7]Department of Land of Israel Studies and Archaeology, Bar-Ilan University, Ramat-Gan 52900, Israel. Corresponding author. Email: elisabetta.boaretto@wiezmann.ac.il.

acid and alkali used vary between laboratories. Bird et al. (1999) introduced the use of wet oxidation as the last step of the chemical pretreatment in charcoal (ABOX). The rationale behind this approach is to remove the "oxidizable" organic carbon, using a mixture of acid-dichromate ($K_2Cr_2O_7$) and sulfuric acid (H_2SO_4), to obtain the most "oxidation-resistant elemental carbon" (OREC).

This study examines the structural and chemical changes that the ABA treatment induces on fossil charcoal samples from the Middle Paleolithic-Upper Paleolithic (MP-UP) transition strata in Kebara Cave, Israel. Interestingly, these charcoal samples have also experienced pH fluctuations (acidic paleo-pH followed by neutral pH) in the past after deposition in the sediments (Schiegl et al. 1996; Karkanas et al. 2000; Shahack-Gross et al. 2004). Thus, the aim is to characterize structural changes in the charcoal when it is exposed to fluctuating pH conditions, and by so doing obtain insights both into what happened to the charcoal in the sediments and when the ABA pretreatment regime is applied during sample preparation for ^{14}C analysis. This could also lead to the identification of quality control criteria for the selection of samples that are more likely to be effectively decontaminated, and are therefore more appropriate for dating. We can also envisage using this information to adopt a tailormade approach to sample preparation for each sample depending upon its state of preservation.

Kebara Cave was chosen as the site for this study because the deposits from the transition from the Middle to the Upper Paleolithic contain abundant charcoal, and the cave's complex stratigraphy has been studied in detail (Laville and Goldberg 1989; Goldberg and Laville 1991; Bar-Yosef et al. 1996; Meignen et al. 2008). In addition, the history of pH fluctuations in this part of the cave has been reconstructed from preserved authigenic phosphate minerals (Schiegl et al. 1996; Karkanas et al. 2000), and most important, a comprehensive dating study involving both ^{14}C and thermoluminescence was carried out on this section (Bar-Yosef et al. 1996). An interesting aspect of charcoal preservation in Kebara Cave is that there is a rough anti-correlation between the distribution of bones and calcitic ash and charcoal in the caves (Karkanas et al. 2000). Very little charcoal is preserved in the northern part of the cave, where calcitic ash and authigenic carbonated apatite are preserved. Abundant charcoal is present in the southern section of the excavated area in the cave, where the sediments do not contain calcite or carbonated apatite, but only the more insoluble phosphate minerals. This includes one of the most insoluble phosphate minerals known from caves, taranakite (Taylor and Gurney 1961), which forms at or below pH 6 depending on the soluble phosphorous or aluminum contents (Karkanas et al. 2000).

The charcoal samples used in this study were from the southern part of the cave. As there was no need to initially remove the more soluble minerals with the first acid treatment, we exploited this fact to compare the ABA treatment with only a BA treatment, in order to better understand the changes in charcoal structure due to fluctuating pH conditions. In addition, we investigated the possibility of removing material with only water before the ABA and BA treatments. We also compared these fossil samples with modern charcoal using 4 different chemical treatments. We compared the fossil samples to a modern charcoal sample produced from oak (*Quercus calliprinos*). This sample was made in an open fire on a clean rocky substrate, and was studied in detail by Cohen-Ofri et al. (2006). Oak was previously identified as one of the common wood types used for fuel in Kebara Cave (Baruch et al. 1992).

EXPERIMENTAL PROCEDURES

Materials

Freshly excavated charcoal specimens from the southern section in Kebara Cave, Israel, were obtained in the spring of 2006 especially for this study. Charcoal specimens from the various

observable layers were not pooled, and great care was taken to differentiate between original deposits (some hearths *in situ* or more consolidated and often layered deposits) and subsequently burrowed deposits (loose homogenized sediment). The latter can comprise more than 50% of the volume of the section in some areas (Laville and Goldberg 1989). The samples were obtained from the south profile of the cave from strata III, IV, and V. Strata III and IV are from the Upper Paleolithic and stratum V mostly from the Mousterian, but close to the MP-UP boundary (Bar-Yosef et al. 1992). Each charcoal sample was placed in aluminum foil, avoiding contact with bare hands, and samples were air dried within a few days after excavation. The samples were then stored at room temperature in aluminum foil. Furthermore, as we cannot exclude the possibility that oxidation of charcoal occurs after excavation and direct exposure to air, we only used fresh samples excavated in June 2006.

Four relatively large fossil samples were chosen for analysis in this study. Table 1 shows the stratigraphic units and squares from which they were derived. Type-1 Reagent Grade Nanopure Water (Barnsted Int.®) and freshly prepared solutions (both acid and alkali) were used throughout the experiment. Modern charcoal from the oak (*Quercus calliprinos*) was produced in an open fire on a clean rocky substrate. After removing the ash by sieving, the charcoal was homogenized by light grinding.

Table 1 Fossil charcoal samples analyzed in this study. Provenience notation follows Laville and Goldberg (1989), Goldberg and Laville (1991), and Bar-Yosef et al. (1996).

Sample name	Stratigraphic unit	Location	Major mineral components
R-16cIIIb	IIIb	R16, x 95, y 25, z 522	Siliceous aggregates
R-17aIIIb,f	IIIb,f	R17, z 511-520	Siliceous aggregates
R-19aIV	IV	R19, z 548-552	Siliceous aggregates
R-19aV	V	R19, z 578-590	Siliceous aggregates

Methods

Specimens were first homogenized by light crushing using an agate mortar and pestle, then sieved through a 250-mm mesh sieve. Batches of ~150 mg were placed in glass tubes and were subject to 4 different types of chemical treatments: 1) acid-base-acid (ABA); 2) base-acid (BA); 3) water-acid-base-acid (H_2O + ABA); and 4) water-base-acid (H_2O + BA). The experimental conditions for each chemical treatment were as follows: a) Initial acid treatment: 3 mL 1N HCl solution (pH 1) for 1 hr, followed by rinsing with Nanopure water until reaching pH 6 (this is the measured pH of the purified water), and then slow drying in an oven at 80 °C; b) Base treatment: 3 mL of 0.1N NaOH solution (pH 14) for 1 hr, followed by Nanopure water rinsing to pH 6 and drying; c) Final acid treatment: 3 mL of 1N HCl solution for 1 hr in a hot water bath at 80 °C, water rinsed to pH 6 after cooling down the pretreated solution to room temperature and drying; d) Water treatment: 3 mL of Nanopure water for 1 hr, followed by centrifugation and drying. Drying in an oven at 80 °C overnight was added in order to determine the weight loss after each step. This is not done in normal sample preparation for ^{14}C. In all cases, the alkaline treatment was repeated 3 times before the final acid treatment. The glass tubes for the chemical treatments were previously cleaned in chromic acid, rinsed, and dried in an oven at 150 °C. At the beginning of every treatment, the samples were agitated for about 30 s to mix and were left to settle for the rest of the treatment at room temperature. In addition, samples R-17aIIIb,f and R-19aIV were subjected to a fourth NaOH treatment after the final acid treatment to further investigate the chemical changes due to alkaline solution exposure. The conditions of centrifugation were kept constant at 3000 rpm for 5 min for acid treatments and 15 min for alkaline treatments, to ensure efficient separation of the insoluble sample from the dark-brown colored supernatant. It should be noted that for all samples and for all 3 alkali treatments, the supernatants

had a dark brown color. After drying overnight in an oven at 80 °C and cooling down to room temperature, weight losses were noted after each chemical treatment. The supernatants from each NaOH treatment were also collected, and dissolved material was precipitated by adding 4 mL of 1N HCl solution, centrifuged, rinsed once, dried, and weighed.

Thermal Analysis

Differential thermal analysis (DTA) and thermogravimetric analysis (TGA) were simultaneously obtained using a TA instruments SDT 600 analyzer and Universal Analyzer (TA Instruments, New Castle, Delaware, USA) data processor software. Thermal decomposition and mass loss at a constant heating rate were measured in the range from room temperature to 1000 °C with an oxygen inlet flow of 100 mL/min and a heating rate of 10 °C/min. High-purity alumina crucibles were used both for sample and reference pans, using loads of 3 mg in a powder form.

Fourier Transform Infrared Spectroscopy (FTIR)

About 0.1 mg of sample was lightly ground in a previously cleaned and dried agate mortar, and then mixed and further ground with 50 mg of dry KBr (Sigma-Aldrich Inc., 99+% FT-IR grade purity) powder. The mixture was pressed into thin, transparent pellets 0.7 cm in diameter with a manually operated press. Scans were obtained in absorbance mode, ranging from 250 to 4000 cm^{-1} with a scanning resolution of 4.0 cm^{-1} using a Nicolet™ 380 spectrometer and OMNIC data processing software.

Transmission Electron Microscopy (TEM)

The samples were prepared as follows: 1 mL of ethanol was added to 1 mg of sample and sonicated (Heat Systems-Ultrasonics Inc., Farmingdale, New York, USA) for 3 min to break the sample up into smaller particles. After settling for ~2 min, 1 drop of the supernatant close to the surface was placed on a carbon-coated copper TEM grid. Excess solution was removed with filter paper. The samples were examined using a 120-keV Philips CM-120 microscope equipped with super-twin objective lenses, a tungsten filament, and an energy dispersive x-ray spectrometer (Phoenix Micro Analyzer [EDAX]). In selected cases, further analyses were made with a Philips-FEI Tecnai F30 microscope, operating at 300 keV, equipped with an electron energy loss spectrometer (EELS) detector.

RESULTS

Here, we report the results of the analyses of 4 different fossil charcoal samples. Where appropriate, we compare these results with a modern charcoal sample treated in the same manner. For more information on this sample of modern charcoal, see Cohen-Ofri et al. (2006).

Effect of pH on Charcoal

In our experimental ABA protocol, 3 successive treatments with alkali are made after an initial treatment with acid, irrespective of the color of the supernatant obtained. The final treatment is again with acid. Infrared spectra of the 4 fossil charcoal specimens, before any treatment, are shown in Figure 1A. They are all very similar. Initially, both carboxylate (COO^-) and carboxylic acid (COOH) groups are present, with the former being the predominant form. The sharp peak at 1384 cm^{-1} in spectra b and d is from sodium nitrate. After HCl treatment, COOH becomes the predominant form, and after alkali treatment, COO^- becomes the predominant form. The charge is presumably neutralized by the presence of cations (counter-ions like sodium). To illustrate this behavior, infrared spectra of sample R-17aIIIb,f are shown in Figure 1B for each treatment stage of the ABA protocol.

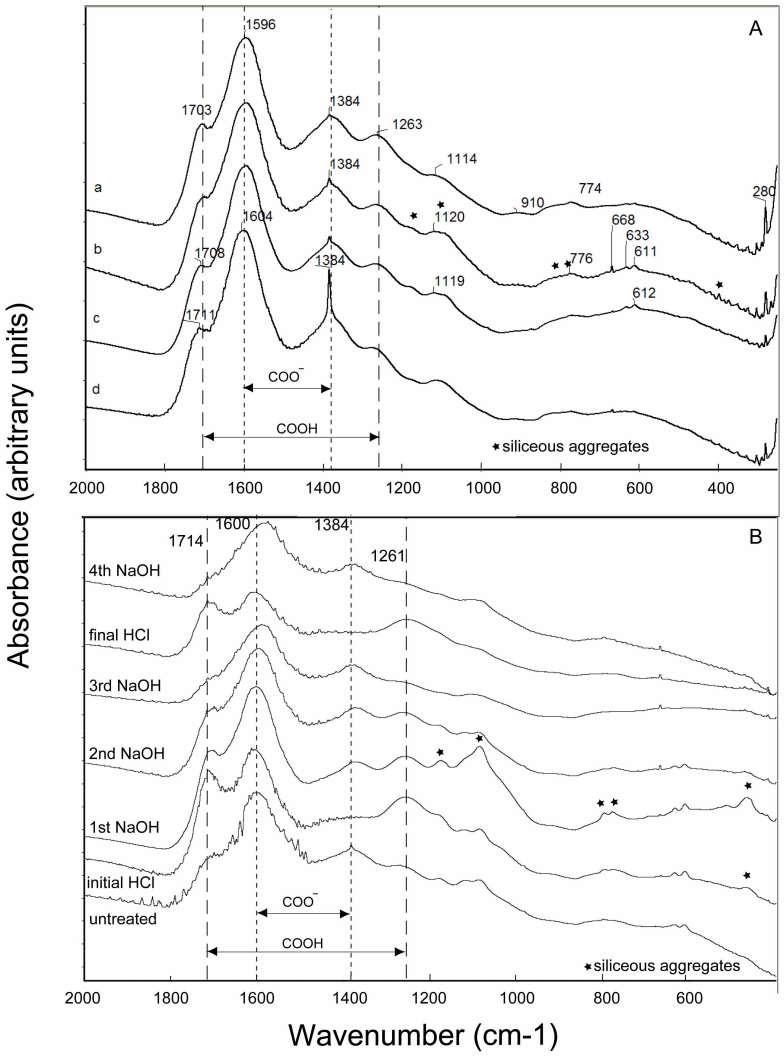

Figure 1 FTIR spectra for A) the 4 fossil charcoal specimens before any treatment: a) R-16cIIIb; b) R-17aIIIb,f; c) R-19aIV; d) R-19aV. B) Sample R-17aIIIb,f before any treatment and after each chemical treatment using the ABA protocol plus an additional final alkali treatment. The arrows point to the COO^- and COOH peak positions indicated by the dotted vertical lines: 1714 and 1261 cm^{-1} for COOH and 1600 and 1384 cm^{-1} for COO^-, respectively. The asterisks show the peaks ascribed to siliceous aggregates that are present in wood.

Thermal Decomposition Upon Heating

In differential thermal analysis/thermogravimetric analysis (DTA/TGA), the sample is slowly heated to 1000 °C and the weight changes as well as the temperature differences relative to an inert reference are measured. The thermal decomposition of constituents of the sample can be then identified by their individual mass losses as they are heated in the presence of oxygen. Figure 2A shows the DTA results of the insoluble fraction after each treatment for sample R-17aIIIb,f. Similar profiles were observed in the other 3 samples, and the specific decomposition temperatures are shown in Table 2. For practical purposes, in this study the maxima of each distinguishable curve are

assumed to be separate fractions, as suggested by Kucerík et al. (2004). Perhaps the most striking observation is that the insoluble fractions after both the initial and final HCl treatments usually exhibit only 1 broad exothermic peak from 400 to 500 °C, whereas the 3 alkaline-treated samples have several fractions both at lower and higher temperatures compared to the sample after HCl treatment. The exception is sample R-16cIIIb, for which 2 fractions can be distinguished within this temperature range after both HCl treatments (Table 2). The TGA/DTA analyses show that the major charcoal components dissociate at low pH and associate into various complexes at high pH. We also note that the highest temperature fractions around 800 °C (Table 2) are not present after the final HCl treatment, but only when the sample is again treated with alkali (Figure 2B).

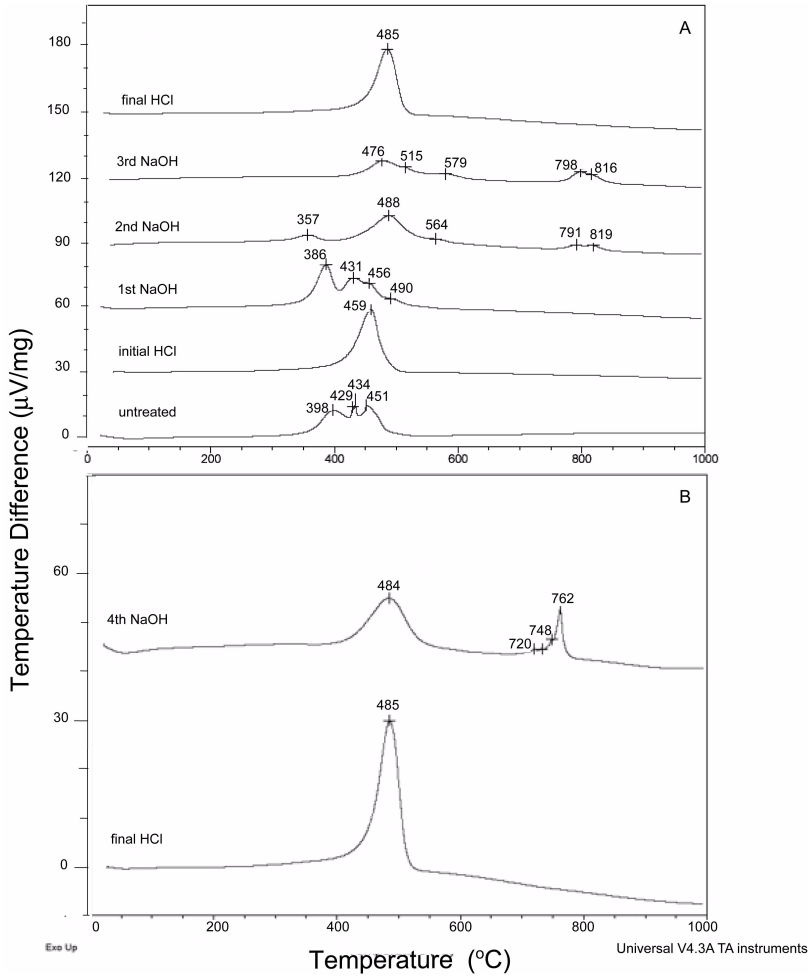

Figure 2 DTA scans for sample R-17aIIIb,f. A) Before any treatment and after each chemical treatment using the ABA protocol. B) Comparison of the final HCl stage with a fourth alkali treatment after the final HCl treatment. The maxima associated with each peak are marked with crosses as well as their corresponding temperatures. These are listed in Table 2 for all 4 samples.

Support for this mechanism of association/disassociation is shown in Table 2. After the last HCl treatment, little or no residue remains after heating to 1000 °C, whereas after alkali treatment resi-

Table 2 Peak maxima from DTA scans for samples treated with the ABA protocol. Values in parentheses are the percentage weight loss for that particular phase change. The values in bold are the fractions associated with the highest mass loss.[a]

Sample	Untreated	Initial HCl	1st NaOH	2nd NaOH	3rd NaOH	Final HCl
R-16cIIIb	**403 (33)**	**445 (40)**	360 (14)	**466 (42)**	**469 (48)**	492 (38)
	443 (24)	456 (29)	**474 (51)**	578 (8)	577 (1)	**513 (40)**
				921 (5)	901 (6)	
R =	18	0	11	13	17	0
R-17aIIIb,f	**398 (30)**	**459 (55)**	**386 (30)**	357 (10)	**476 (20)**	**485 (74)**
	429 (10)		431 (20)	**488 (30)**	515 (8)	
	434 (10)		456 (10)	564 (10)	579 (6)	
	451 (15)		490 (10)	791 (5)	798 (7)	
				819 (5)	816 (13)	
R =	15	14	7	13	17	4
R-19aIV	**418 (25)**	**447 (47)**	395 (30)	347 (9)	343 (10)	**484 (70)**
	448 (10)		**427 (50)**	**476 (45)**	**480 (37)**	
	471 (20)		448 (14)	565 (11)	564 (9)	
					602 (4)	
					803 (7)	
R =	17	10	2	13	5	0
R-19aV	374 (23)	**435 (58)**	369 (28)	349 (12)	522 (15)	**511 (68)**
	468 (32)		**470 (38)**	**477 (35)**	628 (15)	
			561 (3)	552 (7)	752 (3)	
				758 (2)	**771 (23)**	
R =	22	16	15	32	21	5

[a]The rows labeled "R" are the residual mass loss (in %) after burning up to 1000 °C. In all cases, the mass balance to complete 100% is the water loss below 300 °C.

dues comprising about 10–15% of the original weight remain. As the only source of material for this residue is sodium hydroxide, we assume that the heated product is a sodium salt that easily dissolves in HCl, or perhaps sodium hydroxide itself. Thus, the charged form of charcoal is loaded with abundant counter-ions of sodium.

For the modern charcoal sample, the thermal decomposition is around 540 °C (Table 3 in Cohen et al. 2006). The broad peak around this temperature is not significantly modified by exposure to low and high pH solutions.

Microstructural Characterization of Charcoal

The basic structural motif consistently found in all samples examined in the TEM is a combination of microcrystalline graphite-like crystallites surrounded by a less structurally organized (non-diffracting) material. These general features are in agreement with previous reports of the structure of untreated charcoal samples from Kebara Cave (Cohen-Ofri et al. 2006). We observed that the mixed structure is not present in all stages of treatment: after every HCl treatment the micrographs show mostly a uniform, non-organized material (Figures 3C,D); whereas after the NaOH treatments the material is composed of a mixture of microcrystalline structures surrounded by the less organized, semi-ordered material (Figures 3A,B,F). After several NaOH treatments, the proportions of graphite-like crystallites were found to decrease compared to the untreated samples.

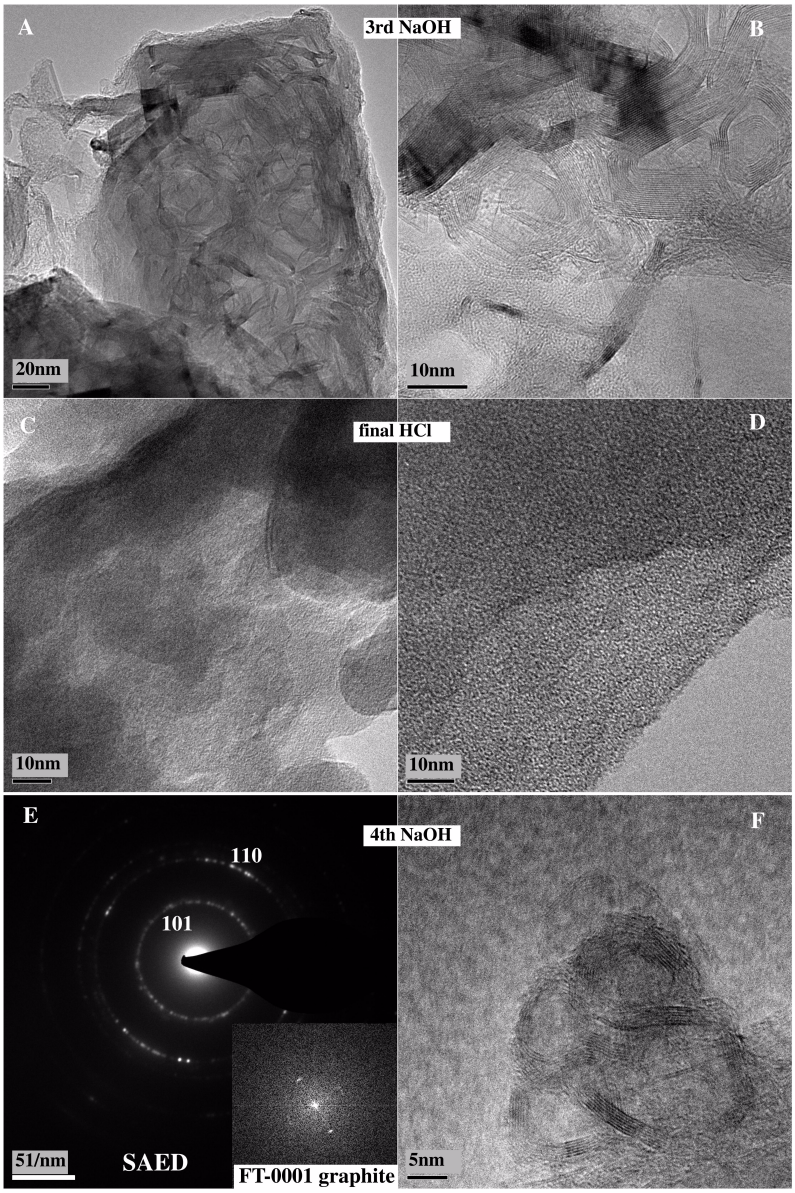

Figure 3 Microstructures observed in the TEM of fractions from sample R-17aIIIb,f. A) and B) Bright field images at low and high magnifications after the third NaOH treatment. C) and D) Bright field images at low and high magnifications after the final HCl treatment. E) Selected area electron diffraction (SAED) pattern from the structure shown in (F) prominently showing 2 reflections of graphite (101 and 110) and (inset) the Fourier transform corresponding to the 0001 plane of graphite (0.35 nm spacing). F) Bright field image of a rounded structure observed after the fourth NaOH treatment.

We do note a correlation between the pH of the treatment and the constituents observed in TEM. A broad band in the DTA profile is in all cases associated with a non-organized material in TEM; conversely, the separation into well-differentiated constituents in DTA is in all cases associated with a

mixture of microcrystalline substructures and the non-organized material in TEM. To illustrate these correlations, micrographs of sample R-17aIIIb,f are shown in Figure 3. After the third alkali treatment, clearly defined microcrystalline layers can be observed (Figures 3A,B) even at relatively low magnification; at this chemical stage, the DTA profile exhibits many fractions spread between 400 and 900 °C (Figure 2A). This same sample after the subsequent acid treatment (Figures 3C,D) exhibits a homogeneous non-organized structure throughout the sample and only 1 broad peak between 400 and 500 °C (Figure 2A). In 1 area of the TEM grid, we did observe lattice fringes identified as graphitic layers (Figure 4) with a spacing that corresponds to the 0001 plane of graphite (0.35 nm). However, the associated DTA spectrum is not different from the other HCl-treated samples. This probably indicates a localized effect that needs to be further studied.

Note that sample R-17aIIIbf, treated once more with alkali after the final HCl treatment, again exhibited the mixture of graphitic layers and non-organized structure. The DTA profile was also again composed of various well-differentiated constituents.

The identification of the graphitic nature of these multilayers was confirmed both by selected area electron diffraction (SAED) patterns (Figure 3E) and electron energy loss spectroscopy (EELS) using high-resolution electron microscopy. The results obtained are similar to those reported by Cohen-Ofri et al. (2007: Figure 4). An additional observation from the comparison between the structure after the third and fourth NaOH was the presence of a much larger amount of graphite-like crystallites in the former (Figures 3B,F). After the third NaOH treatment, the layers seem to spread out evenly and loosely throughout the sample, and after the fourth alkali treatment the graphitic layers seem to be more "tightly" entangled and concentrated in smaller regions. Apart from these differences in morphology, no significant differences were found in the d-spacings from different graphene layers, which ranged from 0.32 nm in highly ordered structures to 0.37 nm in less (semi-ordered) structures.

In 3 of the 4 charcoal samples examined, we identified barite ($BaSO_4$) using TEM, XRD, and FTIR. Barite was absent in the associated sediments based on FTIR. This phenomenon was also observed in certain bones (Trueman et al. 2004).

Weight Loss After Each Acid or Alkali Treatment

In the ABA treatment protocol, only the insoluble pellet is recovered for further treatment and the supernatant is discarded. Thus, after each step a weight loss is incurred. Figure 5 shows the weight losses for all 4 fossil samples and for the modern charcoal subject to ABA treatment. After the first HCl treatment, all 4 fossil samples lose almost the same amount of material. During the successive alkali and final HCl treatments, the weight losses for each sample are different. Significantly, the older the sample, the more material is lost during the treatment procedure. This clearly shows that the 4 samples do have different states of preservation. The amounts of material lost after the entire treatment range from around 50% to more than 90%. A major part of the sample is lost, along with any contaminating material. The modern charcoal sample lost only about 10% of its weight after the initial HCl treatment, and remained unchanged during the alkaline treatments. It again lost some weight after the last acid treatment. Overall, the weight loss for this sample is lower than all the other fossil charcoal samples.

The reproducibility of this experiment was checked for samples R-17aIIIb,f and R-19aIV, for which there was enough sample to repeat the experiment. The weight losses for the ABA treatment were performed twice for each of these samples. The average measurements as well as the standard deviations ($\pm 1\ \sigma$) are shown in Figure 5. Note that the instrument error associated with each measure-

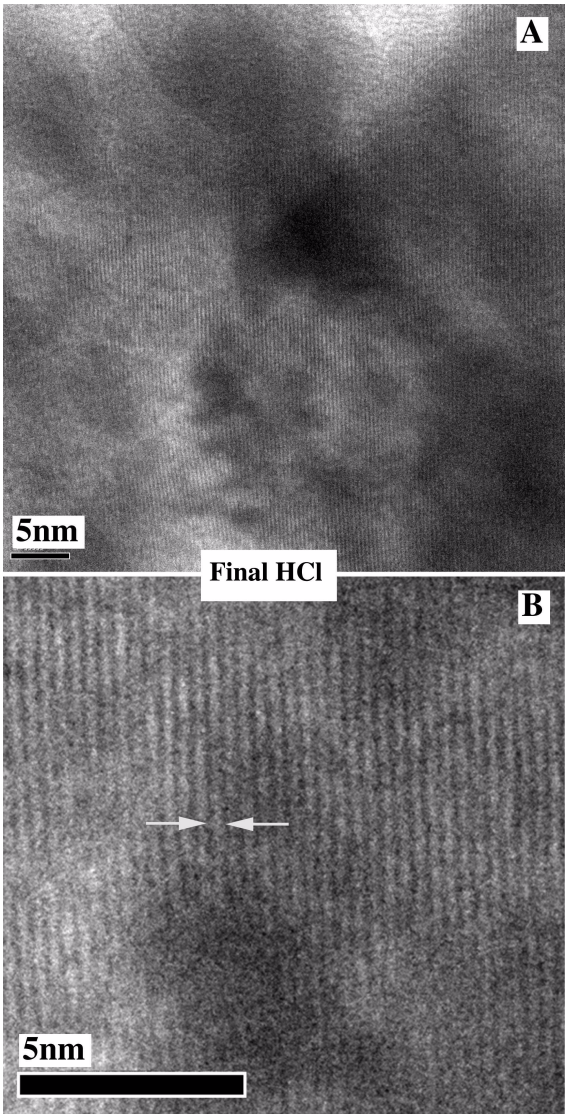

Figure 4 Bright field image of sample R-17aIIIb,f after the final HCl treatment. A) Overview of an area showing a crystalline structure as revealed by the lattice fringes; B) Zoom into image showing lattice fringes spaced by 0.35 nm (marked by arrows), corresponding to the 0001 plane of graphite.

ment is much smaller than the standard deviation. The largest uncertainty values obtained from these calculations were used to assign error bars to the other 2 samples (i.e. R-16cIIIb and R-19aV). Even considering this conservative estimate, the total weight losses from samples in unit III are clearly differentiated from samples in units IV and V.

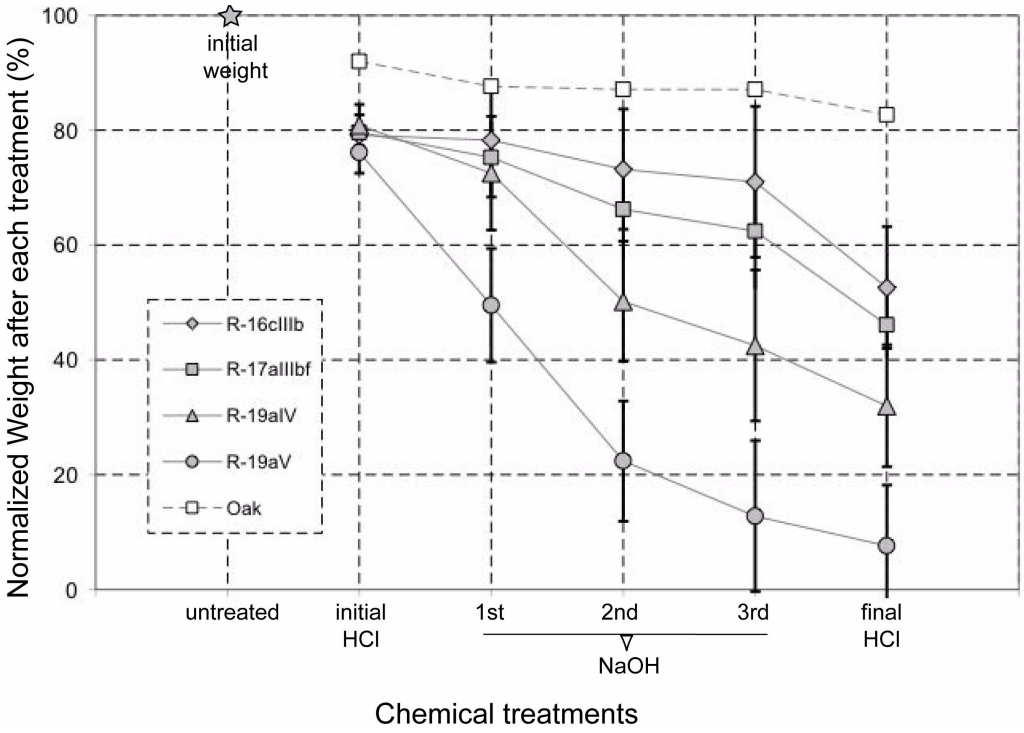

Figure 5 Plot of normalized weights (in percentage) of the insoluble fractions of the 4 fossil samples and modern charcoal (oak) after each chemical treatment for the ABA protocol. The error bars for each data point are the standard deviations (±1 σ).

Comparison of Different Treatment Regimes

As carbonate or relatively soluble phosphate minerals were not present in the charcoal and associated sediments, there was no compelling reason to initially treat the samples with HCl. We therefore compared several different treatment regimes: BA – excludes the first HCl treatment; H_2O-ABA – water is used in addition to the first HCl treatment; H_2O-BA – water is used instead of the first HCl treatment. Figure 6 shows the results for sample 19aIV and for modern charcoal. The weight losses observed for the fossil charcoal (Figure 6A) are as follows: omitting the initial HCl treatment (BA protocol) reduces the weight loss after each treatment. An initial treatment of the sample only with water results in a 13% weight loss. If this is followed by the ABA protocol, the sample still loses most of the material. If, however, the water treatment is followed by the BA protocol, the weight loss is the same as the BA protocol itself. We conclude that the initial acidic pH treatment must cause a major structural reorganization of the sample, presumably because the counter-ions are lost. The same weight loss trends were observed for the other 3 samples. The extra treatment with water does not change the observation that the extent of weight loss corresponds to the age of the samples.

The modern charcoal sample (Figure 6B) exhibits a much lower weight loss than the fossil charcoal samples for all 4 chemical treatment regimes. However, it does exhibit some weight loss, mainly after water and acid treatments. This observation indicates that the acidic pH treatment could also affect the structural reorganization of the sample even when it is in a pristine condition. For the modern sample, the soluble extracts were always clear and no colored (humic) substances were released.

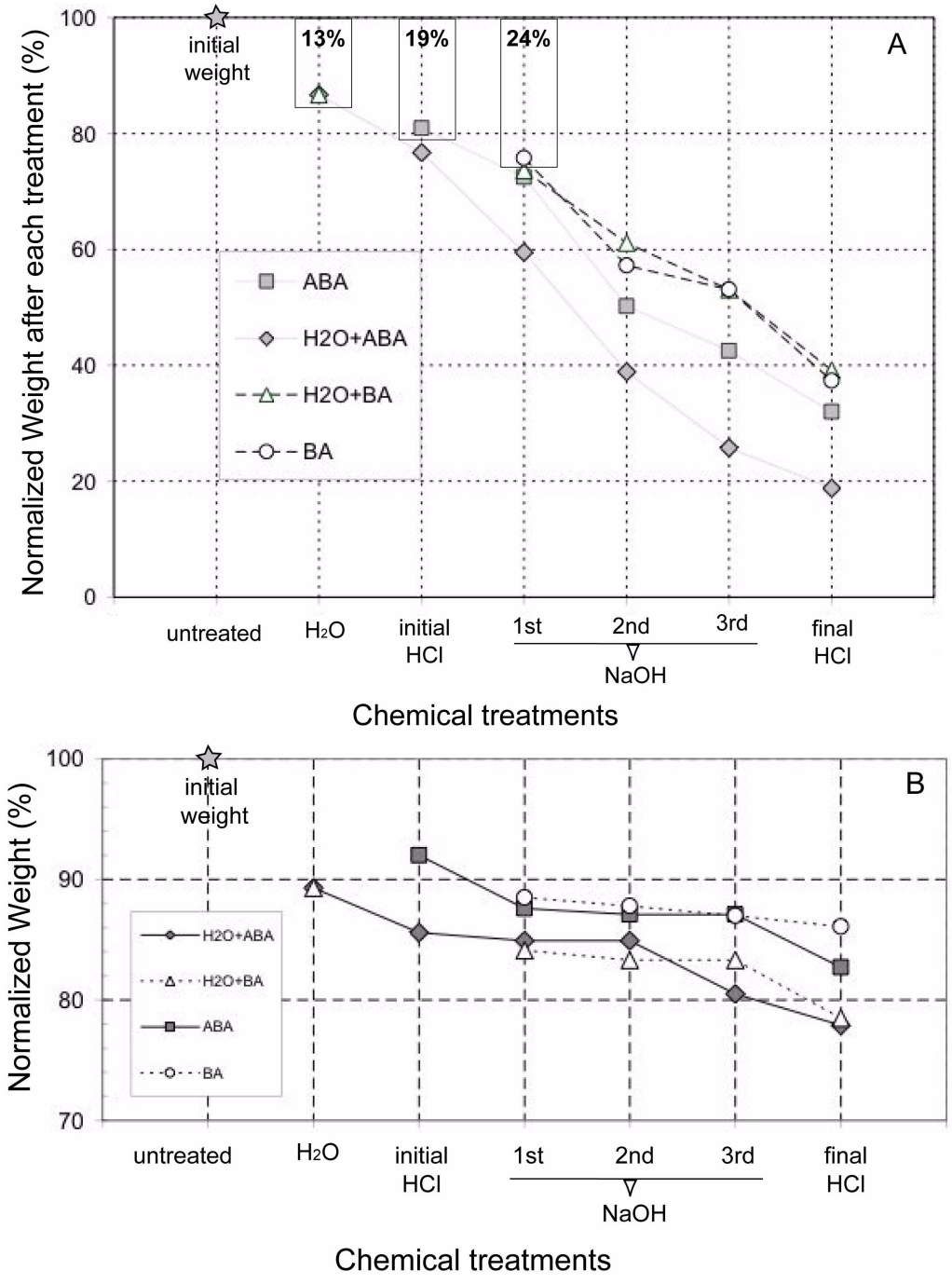

Figure 6 Plot of weights (in percentage) of the insoluble fractions of samples R-19aIV (A) and modern oak charcoal (B) after every step for 4 different chemical treatments: 1) acid-base-acid (ABA); 2) base-acid (BA); 3) water-acid-base-acid (H_2O + ABA); and 4) water-base-acid (H_20 + BA). Error bars are not included in this chart for clarity purposes.

We also examined the weights of the supernatants recovered after the various NaOH treatments in fossil charcoal samples. For the ABA-treated samples, the weights of the material recovered after precipitation (with HCl), rinsing with water, and drying were very similar to the weight loss of the sample after the corresponding NaOH treatment. However, this was not the case for the BA-treated samples; only ~60% of the weight loss was recoverable from the supernatant by adding HCl, rinsing, and drying. The rest presumably remained in the solution. This too shows that the initial exposure to an acid environment changes the extent to which the insoluble components dissolve in subsequent alkaline solutions. Furthermore, the differences in weight losses between the ABA- and BA-treated samples are intimately related to the initial effect of HCl on the COO^- groups.

DISCUSSION

Here, we establish that fossil charcoal subject to pH fluctuations *in vitro* is significantly modified. The acid treatment disrupts the structure and results in a fairly homogeneous product, whereas the treatment with alkali results in a heterogeneous product. Significant weight losses are incurred after different treatments, with the greater losses occurring in the older samples. Initial treatment with water also results in a significant weight loss. The following is a discussion on how acid and alkali treatments may affect the structural stability of fossil charcoal both *in vitro* and in nature.

Stability of Fossil Charcoal

The basis for understanding the effects of exposing fossil charcoal to high and low pH solutions is to first understand as much as possible about the factors that are responsible for stabilizing fossil charcoal prior to any treatment. We identify 2 structural features responsible for stabilizing fossil charcoal: graphite-like crystallite stacks and carboxylate-mediated salt bridges linking molecules.

In modern charcoal and well-preserved fossil charcoal, graphite is a major component. Thus, the electronic interactions governing the stacking of graphene layers may be the major stabilizing factors. These are predominantly attractive long-range van der Waals forces (van der Waals 1873) interacting with net repulsive short-range weak chemical interactions from the graphene layers (Dappe et al. 2006).

Cohen-Ofri et al. (2007) established that fossil charcoal is likely to degrade by oxidation, as inferred from the presence of carboxylate groups in fossil charcoal that are not originally present in pristine charcoal. In fact, oxygen is not present in significant quantities in modern charcoal (Cohen-Ofri et al. 2007). Two mechanisms of oxidation of fossil charcoal were proposed by Cohen-Ofri et al. (2006): 1) breakdown of the graphitic component through oxidative attack at defect points; and 2) oxidation of the non-organized component[8] to form carboxyl groups. By implication, the rounded onion-like structures preferably found in fossil charcoal are the most stable phases, presumably because the lack of exposed edges and/or defects minimizes oxidative attack.

The carboxyl groups may exist in 2 states: carboxylate ($RCOO^-$) and carboxylic acid (RCOOH) groups. Infrared spectra (Figure 1) show that both are present in the Kebara charcoal samples examined. The proportions in which they are present are determined by the acid dissociation constant K_a, defined as the concentration ratio between the reactants available ($RCOO^- + H^+$) and the reaction products (RCOOH) when the system reaches its lowest energetic state. This K_a constant is directly

[8]Here, we use the term "non-organized structure" in a broader sense than the "non-organized phase" defined by Franklin (1951) as the non-graphitizable carbon. We also refer here to "non-organized" structure as all non-diffracting material that may or may not contain carbon.

related to the pK_a parameter ($pK_a = -\log_{10}K_a$), which determines the pH range where partial dissociation can take place. This in turn is a function of the microenvironment in which each carboxyl group is located within the charcoal structure. Thus, the initial relative proportions of RCOOH and $RCOO^-$ groups can be regarded as the steady state reached in time under certain pH conditions. Moreover, in order to maintain a balance in the electronic charge, the $RCOO^-$ groups form complexes linked by counter-ions. This in turn can form "salt-bridges" between molecules. Their presence presumably contributes to the stability of the fossil charcoal structure.

Contaminants

The fossil charcoal adsorbs contaminants from the surroundings. These can be ions, small organic molecules, and large polymers such as humic substances that form in soils. If the charcoal is well preserved, then it will have a high proportion of graphite-like crystallites with hydrophobic surfaces. If the fossil charcoal is poorly preserved, then it will be dominated by charged molecules and hence have more hydrophilic surfaces. Thus, the contaminants that adhere to well-preserved and poorly preserved charcoal may be different. Therefore, removing the contaminants from fossil charcoal may be more effective if the preservation state of the charcoal is taken into account.

Humic substances will readily adsorb to fossil charcoal, and especially to poorly preserved fossil charcoal, as they too contain abundant carboxylate groups particularly in the non-organized structure rather than the less-charged graphite phase. It can be assumed that as these contaminants are transported through the groundwater, they are likely to be relatively hydrophilic and have low molecular weights compared to the bulk of the soil humic substances. It is interesting to note that when the Kebara charcoal samples were treated only with water, more than 10% weight loss occurred. It would be interesting to determine if this included a significant amount of the contamination, bearing in mind that it was probably water-soluble to start with.

The high temperature fractions around 800 °C observed only after the third and fourth alkali treatments (Figure 2B) are likely to be concentrated throughout the treatment presumably because they are consistently insoluble in the solutions used, relative to the other components in the sample. These fractions could be organic or inorganic compounds with high thermal stability.

Exposure to an Acidic Environment

The first step in the purification of fossil charcoal is to treat the sample with HCl. The ability of natural and highly oriented pyrolytic graphite (HOPG) to accommodate transition metal compounds is well known and has been extensively investigated in order to produce graphite-intercalated compounds (GICs) as synthetic metals and superconductors (Pietronero and Tosatti 1981). Kang et al. (1998) reported that exposure of natural graphite to an aqueous solution of hydrochloric acid (HCl), enhances the intercalation of iron chlorides ($FeCl_4$) in between the graphite layers. The HCl preferentially attacks defect sites and its effect is optimal at a concentration of 1M. Schlögl (1987) used X-ray photoelectron spectroscopy to demonstrate that the graphitic (0001) surface of highly oriented graphite is irreversibly chlorinated (intercalated with chlorine compounds) at room temperature. We therefore infer that treatment with 1N HCl causes major structural changes in the stacking of graphene layers in fossil charcoal. This inference is supported by the observed weight loss in modern charcoal, for which the state of preservation is optimal and where the proportion of graphite-like crystallites is much higher than in fossil charcoal as suggested by Cohen et al. (2006). We also noted that α-graphite (Alfa Aesar 99.9% purity) exposed to 1N HCl in a hot bath at 80 °C exhibits a broadening of the DTA transition curve around 775 °C compared to untreated graphite—an indication of disruption of the graphite structure upon exposure to HCl. The treatment with acid also results in the

exposed carboxylate groups losing their counter-ions and becoming protonated to form carboxylic groups. Thus, the salt bridges between molecules in the fossil charcoal will be affected, and this will be especially dramatic for poorly preserved charcoal that has relatively few stacked graphite-like crystallites. The result of this structural rearrangement can be seen qualitatively in the TEM, where all the material appears dispersed and uniform. In the DTA, most of the HCl-treated samples exhibit an arrangement of components with very similar thermal stabilities, spreading over a small temperature range. The dispersion in the microstructure is thus consistent with the thermal stability homogenization, but the specific underlying mechanisms for structural dissociation as well as the reasons for homogenization between 400 to 500 °C need to be further investigated.

A significant amount of the sample is lost during this treatment. This indicates that in this dispersed state the more soluble, presumably low molecular weight materials (primary fossil charcoal constituents and contaminants) go into solution.

Exposure to the First Alkali Treatment

In general, the hydroxyl group is a powerful electron donor that can cause the breakdown of covalent bonds. This would produce low molecular weight compounds that will readily dissolve. We can identify a few different effects that NaOH may have on fossil charcoal structure and stability, based on literature data and our experiments:

a. Dissociation of the uncharged carboxylic groups into charged carboxylate groups as explained in the section regarding the pH effect on charcoal. These will be bound by the only cations available, namely the monovalent sodium ions from the alkali. Thus, the salt bridges will be significantly weaker (e.g. upon further HCl treatment) than those that were present in the original charcoal, which we assume included divalent cations as well.

b. Graphite pretreated with alkali is more susceptible to oxidation at high temperatures (700–800 °C). The salts either modify the reaction with the oxygen (Wieber et al. 2006) or produce new active sites on the basal plane for oxygen to attack. For the latter, a model was proposed (Moulijn and Kapteijn 1995), where the sodium ions associate with the oxygen ions and, acting as a complex, attach to the carbon lattice and weaken the C-C bonds. The overall result is an enhancement of the oxygen attack on the graphite and desorption of carbon oxides. Such an effect may be important when step combustion is performed on charcoal samples to separate the more oxidizable material.

c. Purification of graphite by the alkali digestion method (Rao and Patnaik 2004). This process is based on the solubility of various forms of silicates in NaOH at different temperatures. The silicates dissolve in a 12.5M sodium hydroxide solution, but the graphite remains. Consistent with this argument, we do observe a reduction in the signal from the siliceous aggregates upon chemical treatments (Figure 1B).

All these effects or part of them could account for the tendency in the DTA curves for the major insoluble phase after alkali treatment to be more stable and hence transform at a higher temperature, as the lower molecular weight fractions are lost. The presence of the sodium counter-ions and the charged nature of the relatively poorly preserved Kebara charcoal samples will also result in different complexes interacting with each other to produce more or less stable aggregates. This too is consistent with the presence of several well-separated transitions in the DTA spectra spread over a larger temperature range after NaOH rather than after HCl treatments.

For modern charcoal, the observed weight loss after the first alkali treatment is likely to be due mainly to the breakdown of covalent bonds, since there are almost no carboxyl groups in the sample (Figure 9 in Cohen et al. 2006).

The Second and Third Alkali Treatments

The weight loss curves clearly show that more material is lost in the second and third alkali treatments. This means that the remaining insoluble fraction changes with each successive treatment and some material goes into solution. This may well be due to the continued breakdown of covalent bonds, and also perhaps as a result of the opening up and exposure of previously buried carboxylate groups.

Remarkably, the color of the soluble fraction for all 4 fossil charcoal samples during the second and third NaOH treatments is as dark as the first treatment, even when a clear solution is obtained after repeated water rinsing at the end of each treatment. This raises the question about the ideal number of alkali treatments needed to ensure an effective removal of alkali-soluble contaminants. For the samples initially treated with alkali first (BA treatment), the weight loss reached a plateau after the third treatment, as opposed to the case of the samples treated with the standard ABA protocol. This is probably due to the severe structural changes that the acid treatment has on the charcoal structure.

Contrary to the case of fossil charcoal, modern charcoal did not lose a significant amount of material after the second and third alkali treatments for any of the 4 different chemical treatments. Also, the soluble extract was clear and did not release any humic substances. We infer that for very well preserved charcoal, fewer alkali treatments are needed.

The Final HCl Treatment

This treatment again changes the remaining insoluble material into a dispersed, fairly uniform structure based both on TEM and DTA analysis. However, the temperature of transformation in the DTA is higher than that obtained in the first HCl treatment, presumably reflecting the absence of the lower molecular weight fractions.

Implications for Charcoal Preservation

The natural processes that result in a preferential preservation of charcoal in the southern area of Kebara Cave can be better understood within the context of the structural changes described above. The formation of certain authigenic minerals that are associated with the charcoal in the south of the cave is a clear indication of a paleo-acidic environment (Schiegl et al. 1996). The drop in pH to around 4 or 5, the conditions under which the authigenic mineral taranakite forms (Karkanas et al. 2000), would convert many of the carboxylate groups to carboxylic acids, with the concomitant release of the counter-ions. Some of these counter-ions, such as iron and manganese, are known to act as catalysts that facilitate the oxidation of graphite (Chernysh et al. 1993). Their removal from the charcoal after the pH drop could thus have contributed to the preservation of charcoal in the south, whereas in the north of the cave where the pH drop did not occur, the charcoal could have rapidly oxidized and disintegrated. A study of the bat guano degradation processes indicates that the acidic environment was likely to have formed soon after burial (Shahack-Gross et al. 2004). Thus, the effect may have been enhanced as recently buried charcoal is expected to still contain a relatively large proportion of graphite-like crystallites.

Once most of the organic matter was degraded, the sediment around the charcoal became less acidic and eventually returned to neutral or slightly alkaline conditions. The carboxylic acids (RCOOH) would then revert to carboxylates, and the newly introduced counter-ions could form salt bridges that would stabilize the charcoal. These, however, are less likely to include the transition metals, such as iron and manganese, as they are generally not soluble at neutral pH.

The reasons for the differential preservation between different units within the southern area of the cave are more elusive. The fact that the older charcoal samples are more degraded suggests that the degradation process is slow and ongoing, and that thermodynamic equilibrium has not been reached.

We note that in the laboratory, acidic conditions tend to destabilize the charcoal. We assume that this is due to the much higher concentration of acid in 1N HCl as compared to the conditions in the sediments.

Implications for Charcoal Purification

The ABA treatment has certainly proved to be generally effective for removing contaminants from charcoal. This is probably because the acid and the alkali treatments are harsh, and if the charcoal is sufficiently stable to withstand the treatment, then the contaminants are effectively removed. Problems arise when the charcoal is not sufficiently stable and disintegrates and/or dissolves during the treatment. Furthermore, poorly preserved charcoal may also be more likely to absorb water-soluble contaminants. This study raises a series of questions that could be systematically addressed regarding changes in the ABA protocol that might be advantageous for purifying poorly preserved charcoal:

1. Is it possible to use a more dilute solution of HCl that will still dissolve the carbonates that may be associated with the charcoal, but be less damaging to the charcoal structure? The 1N HCl clearly disrupts the charcoal structure, and could conceivably expose new surfaces that bind the contaminants even more tightly.
2. Is it necessary to start with an acid treatment, or is it sufficient to only end with an acid treatment to remove the carbonates and the modern absorbed carbon dioxide? The weight losses incurred during the BA treatments showed that material was removed to a similar extent as with the ABA treatment. Although some contaminants may be removed by the initial acid treatment, the formation of carboxylic acid groups in the contaminating humic substances probably makes them more insoluble.
3. Are contaminants removed during the first water treatment? A significant weight loss did occur after treating the original charcoal with water. It is conceivable that water-soluble contaminants might be effectively removed in this simple procedure, without causing major structural changes.
4. Is it necessary to perform repeated alkali treatments? Our protocol involves initially agitating the sample after adding the alkali and then letting the sample stand for 1 hr. The extraction of contaminants might be more effective if the sample was kept in motion on a rocking table, as the effectiveness of the alkali would not be diffusion limited.

It would be most advantageous to have a simple prescreening method that could identify poorly preserved charcoal, then the cleaning protocol could be adapted accordingly. Weight loss is a good indication of the state of preservation, although it is not obvious how this could be used as a simple prescreening method. It would also be very helpful to have criteria for knowing to what extent the sample has been decontaminated. Alon et al. (2002) proposed using fluorescence.

CONCLUSIONS

Insights into the structural stability of fossil charcoal have emerged from this study. In poorly preserved charcoal, the "salt bridges" that serve as links for the carboxylate groups contribute significantly to its structural stability. The type of counter-ions that form these bridges may promote further oxidation or may act as inhibitors. The liberation and potential exchange of these counter-ions with the microenvironment under acidic conditions is a key factor for understanding the preferential

preservation of charcoal in nature once subject to acidic paleo-pH conditions in the sediments. It also provides insight into the changes in thermal and structural stability of charcoal when subject to fluctuating pH conditions *in vitro*. It is anticipated that a thorough understanding of the structural effects of solutions used during purification will enable a tailormade approach for contamination removal and will contribute to more accurate and precise ^{14}C dating.

ACKNOWLEDGMENTS

We thank Delphine Dumarché for her assistance in the fieldwork. This research was funded by Israel Science Foundation grant nr 05/1040. Financial support was also obtained from the Kimmel Center for Archaeological Science at the Weizmann Institute of Science and the American School of Prehistoric Research (Peabody Museum, Harvard University), as well as a generous gift from the late Mr. George Schwartzmann.

REFERENCES

Alon D, Mintz G, Cohen I, Weiner S, Boaretto E. 2002. The use of Raman spectroscopy to monitor the removal of humic substances from charcoal: quality control for ^{14}C dating of charcoal. *Radiocarbon* 44(1): 1–11.

Baruch U, Werker E, Bar-Yosef O. 1992. Charred wood remains from Kebara Cave, Israel: preliminary results. *Bulletin de la Société Botanique de France, Actualitiés Botaniques* (2/3/4):531–8.

Bar-Yosef O, Vandermeersch B, Arensburg B, Belfer-Cohen A, Goldberg P, Laville H, Meignen L, Rak Y, Speth JD, Tchernov E, Tillier A-M, Weiner S. 1992. The excavations in Kebara Cave, Mt. Carmel. *Current Anthropology* 33(5):497–550.

Bar-Yosef O, Arnold M, Mercier N, Belfer-Cohen A, Goldberg P, Housley R, Laville H, Meignen L, Vogel JC, Vandermeersch B. 1996. The dating of the Upper Paleolithic layers in Kebara Cave, Mt Carmel. *Journal of Archaeological Science* 23(2):297–306.

Bird MI, Ayliffe LK, Fifield LK, Turney CSM, Cresswell RG, Barrows TT, David B. 1999. Radiocarbon dating of "old" charcoal using a wet oxidation, stepped-combustion procedure. *Radiocarbon* 41(2):127–40.

Bird MI, Turney CSM, Fifield LK, Jones R, Ayliffe LK, Palmer A, Cresswell R, Robertson S. 2002. Radiocarbon analysis of the early archaeological site of Nauwalabila I, Arnhem Land, Australia: implications for sample suitability and stratigraphic integrity. *Quaternary Science Reviews* 21(8–9):1061–75.

Chernysh IG, Pakhovchishin SV, Goncharik VP. 1993. The activity of dispersed oxides on natural exfoliated graphite surfaces. *Reaction Kinetic and Catalysis Letters* 50(1–2):273–7.

Cohen-Ofri I, Weiner L, Boaretto E, Mintz G, Weiner S. 2006. Modern and fossil charcoal: aspects of structure and diagenesis. *Journal of Archaeological Science* 33(3):428–39.

Cohen-Ofri I, Popovitz-Biro R, Weiner S. 2007. Structural characterization of modern and fossilized charcoal produced in natural fires as determined by using electron energy loss spectroscopy. *Chemistry: A European Journal* 13(8):2306–10.

Dappe YJ, Basanta MA, Flores F, Ortega J. 2006. Weak chemical interaction and van der Waals forces between graphene layers: a combined density functional and intermolecular perturbation theory approach. *Physical Review B* 74:205434-1–9.

Franklin RE. 1951. Crystallite growth in graphitizing and non-graphitizing carbons. *Proceedings of the Royal Society of London A* 209:196–218.

Frink DS. 1992. The chemical variability of carbonized organic matter through time. *Archaeology of Eastern North America* 20:67–79.

Goldberg P, Laville H. 1991. Etude géologique de dépôts de la grotte de Kébara (Mont Carmel): campagnes 1982–1984. In: Bar-Yosef O, Vandermeersch B, editors. *Le Squelette Mousterien de Kébara 2*. Paris: Editions C.N.R.S. p 29–41. In French.

Kang F, Leng Y, Zang T-Y, Li B. 1998. Electrochemical synthesis and characterization of ferric chloride-graphite intercalation compounds in aqueous solution. *Carbon* 36(4):383–90.

Karkanas P, Bar-Yosef O, Goldberg P, Weiner S. 2000. Diagenesis in prehistoric caves: the use of minerals that form *in situ* to assess the completeness of the archaeological record. *Journal of Archaeological Science* 27(10):915–29.

Kucerík J, Kovár J, Pekar M. 2004. Thermoanalytical investigation of lignite humic acids fractions. *Journal of Thermal Analysis and Calorimetry* 76(1):55–65.

Laville H, Goldberg P. 1989. The collapse of the Mousterian sedimentary regime and the beginning of the Upper Paleolithic at Debara. In: Bar-Yosef O, Vandermeersch B, editors. *Investigations in South Levantine Prehistory.* Oxford: BAR International Series 497. p 75–95.

Meignen L, Goldberg P, Bar-Yosef O. 2008. The hearths at Kebara Cave and their role in site formation processes. In: Bar-Yosef O, Meignen L, editors. *Kebara Cave, Mt. Carmel, Israel: The Middle and the Upper*

Paleolithic Archaeology. Part I. Cambridge, Massachusetts: Peabody Museum, Harvard University. p 91–122.

Moulijn JA, Kapteijn F. 1995. Towards a unified theory of reactions of carbon with oxygen-containing molecules. *Carbon* 33(8):1155–65.

Olson EA, Broecker WS. 1958. Sample contamination and reliability of radiocarbon dates. *Transactions of the New York Academy of Science Series II* 20:593–604.

Pietronero L, Tosatti E. 1981. *Physics of Intercalation Compounds*. Berlin: Springer-Verlag. 323 p.

Rao RB, Patnaik N. 2004. Preparation of high pure graphite by alkali digestion method. *Scandinavian Journal of Metallurg*y 33(5):257–60.

Sakamoto M, Kodaira A, Imamura M. 2004. An automated AAA preparation system for AMS radiocarbon dating. *Nuclear Instruments and Methods in Physics Research B* 223–224:298–301.

Schiegl S, Goldberg P, Bar-Yosef O, Weiner S. 1996. Ash deposits in Hayonim and Kebara caves, Israel: macroscopic, microscopic and mineralogical observations, and their archaeological implications. *Journal of Archaeological Science* 23(5):763–81.

Schiffer MB. 1986. Radiocarbon dating and the "old wood" problem: the case of Hohokam chronology. *Journal of Archaeological Science* 13(1):13–30.

Schlögl R. 1987. Modification of the electronic structure of graphite by intercalation, chlorination and ion etching. *Surface Science* 189–190:861–72.

Shahack-Gross R, Berna F, Karkanas P, Weiner S. 2004. Bat guano and preservation of archaeological remains in cave sites. *Journal of Archaeological Science* 31(9): 1259–72.

Taylor AW, Gurney EL. 1961. Solubilities of potassium and ammonium taranakites. *Journal of Physical Chemistry* 65(9):1613–6.

Taylor RE. 1987. *Radiocarbon Dating: An Archaeological Perspective*. Orlando: Academic Press. 212 p.

Trueman CNG, Behrensmeyer AK, Tuross N, Weiner S. 2004. Mineralogical and compositional changes in bones exposed on soil surfaces in Amboseli National Park, Kenya: diagenetic mechanisms and the role of sediment pore fluids. *Journal of Archaeological Science* 31(6):721–29.

van der Waals J. 1873. Over de Continuïteit van den Gas - en Vloeistoftoestand (On the continuity of the gas and liquid state) [PhD dissertation]. Leiden: Leiden University. In Dutch.

Wieber AP, Guzman JE, Wolf EE. 2006. An STM study of phosphoric acid inhibition of the oxidation of HOPG and carbon catalyzed by alkali salts. *Carbon* 44(10):2069–79.

Yizhaq M, Mintz G, Cohen I, Khalaily H, Weiner S, Boaretto E. 2005. Quality controlled radiocarbon dating of bones and charcoal from the early Pre-Pottery Neolithic B (PPNB) of Motza (Israel). *Radiocarbon* 47(2):193–206.